energies

Review

A Survey on the Shortcomings of the Current Rate of Penetration Predictive Models in Petroleum Engineering

Mitra Khalilidermani and Dariusz Knez *

Department of Drilling and Geoengineering, Faculty of Drilling, Oil, and Gas, AGH University of Krakow, 30-059 Krakow, Poland
* Correspondence: knez@agh.edu.pl; Tel./Fax: +48-12-617-3784

Abstract: In drilling engineering, the rate of penetration (*ROP*) is a prevalent indicator to evaluate the energy efficiency of drilling operations. Nowadays, *ROP* prediction has become more critical since the production from deeper hydrocarbon resources is unprecedentedly escalating. So far, a wealth of theoretical and practical investigations has been conducted to develop *ROP* models; however, the existing models have not been adequately updated with the new technological advancements or geological restrictions. This research strives to integrate the latest advancements, restrictions, and future requirements in *ROP* prediction. To do this, the existing empirical and data-driven *ROP* models are elaborated and compared. From the conducted research, it was deduced that four uncontrollable factors, including the rock permeability, wellbore inclination, temperature, and rock hardness, have not been adequately considered in *ROP* models. Moreover, although data-driven *ROP* models deliver more accurate results than the empirical models, the determination of the number and type of the input parameters is still challenging. To tackle this issue, it is recommended to develop a formation-based classification system of input parameters for future investigations. This inclusive review can be adopted by the companies and engineers involved in drilling operations to update and reform their drilling strategies.

Keywords: *ROP*; drilling optimization; wellbore inclination; artificial intelligence; hydrocarbon reservoir; ANN; SVM; rock permeability; rock hardness; petroleum engineering

Citation: Khalilidermani, M.; Knez, D. A Survey on the Shortcomings of the Current Rate of Penetration Predictive Models in Petroleum Engineering. *Energies* **2023**, *16*, 4289. https://doi.org/10.3390/en16114289

Academic Editors: Mohamed Mahmoud and Zeeshan Tariq

Received: 6 April 2023
Revised: 15 May 2023
Accepted: 22 May 2023
Published: 24 May 2023

1. Introduction

How can drilling engineers predict the rate of penetration (*ROP*) more accurately? As the need for the exploitation of deeper hydrocarbons is increasingly growing, are existing *ROP* models still adequately reliable? What factors have been neglected in existing *ROP* models? How can *ROP* models be improved? These questions are constantly exchanged between drilling engineers as they are dealing with the minimizing of total budget and time spent for drilling operations. To access the subsurface natural resources, e.g., oil, gas, groundwater, minerals, etc., drilling is known as the most expensive option [1]. To reduce the cost and time of drilling, usually, drilling engineers optimize the mechanical specific energy (MSE) or the *ROP*. The MSE demonstrates the required energy for breaking the rock, while the *ROP* indicates the pace of drilling operations [2]. In this review article, existing *ROP* models are assessed, together with their shortcomings and future requirements.

From the mathematical perspective, the *ROP* is defined as the ratio of the rock's drilled length to the drilling time. The *ROP* can be affected by a wide spectrum of miscellaneous factors [3]. Those factors are classified as the controllable and uncontrollable factors. The adjustable factors, e.g., revolutions per minute (*RPM*), mud-flow rate (Q), torque (T), and weight on bit (*WOB*), can be changed and controlled by the operators [4]. By contrast, some other factors cannot be changed due to technological limitations, or geological conditions. For instance, wellbore trajectory, pore pressure, rock strength, and equivalent circulation density (ECD), are examples of uncontrollable factors [5].

Since the *ROP* directly influences the entire drilling cost and time, many researchers and companies have had special concerns to model this parameter. To tackle this, the impact of the different contributing factors on the *ROP* have been investigated for decades; however, *ROP* optimization is a sophisticated task as the relations between the *ROP* and different contributing factors are often commonly complicated [6–12]. Therefore, several attempts were made by different researchers to develop high-performance, predictive models to achieve optimal results.

The initial concentration of those studies was on the development of empirical models derived from the experimental tests. The first attempt to optimize drilling parameters was performed by [13]. In that study, an experimental formula correlating the *ROP* with the bit life was established. The factors of *RPM*, *WOB*, and drilling depth were included in the corresponding *ROP* model.

Maurer was the next researcher who offered a mathematical relation to predict the *ROP* for the roller-cone bits [14]. Galle and Wood used a number of graphs and diagrams to develop a method for determining the best association of *WOB* and *RPM* for a special kind of bit [15]. Bingham modified Maurer's model, and proposed an experimental model; however, the drilling depth was not considered in the model, and it was also restricted to low values of *RPM* and *WOB* [16]. At the same time, Teale introduced an empirical correlation linking the *ROP* to the MSE [17]. In that model, the *ROP* was used to determine the necessary energy for drilling of a unit volume of rock. After Teale, Eckle performed several micro-bit experiments, and investigated the impact of overbalance pressure reduction on the *ROP* improvement [18].

One of the most significant investigations dates back to the empirical *ROP* model suggested by Bourgoyne and Young [3]. In such a mathematical model, several drilling parameters were included, and, therefore, it was widely applied as a practical optimization method to adjust the real-time parameters of drilling operations [19]. The next two models belonged to Warren who introduced his first model in [20], and, then, declared a modification of the previous model in [21]. The first model, which was called the "perfect-cleaning model", included the rock strength, bit diameter, *RPM*, and *WOB*. The second model, known as the "imperfect-cleaning model", was based on the first model; however, it included the cuttings removal term. In better words, mud properties, e.g., density and viscosity, and the effect of jet impact force were incorporated in *ROP* modeling. Improvement and development of empirical *ROP* models was then followed by several researchers [22–27].

Apart from the empirical models, some researchers strived to predict the *ROP* using artificial intelligence (AI) algorithms. In fact, numerous data are collected daily during the drilling activities. However, such data are full of uncertainties and hidden correlations that can be well-handled by AI analytical tools [28]. Recently, *ROP* prediction by the AI techniques is one of the most reliable methods delivering acceptable results [29–32]. Some valuable works related to AI-based *ROP* models can be found in [33–43].

ROP models are also applicable in the mining industry. There have been many investigations for *ROP* prediction in mines [44–53]. In the mining industry, drilling operations are executed for implementation of coring boreholes or blasting holes. Comparing the oil/gas wells with mining boreholes, it can be claimed that the *ROP* is more critical in oil/gas drilling operations as the destination depth is far deeper than that of mining activities. Apart from the mining and oil/gas industry, drilling operations are also an indispensable part of some other engineering applications, such as water-well drilling [54,55], coal-bed methane extraction, and extraterrestrial applications [56,57]. Thus, optimization of the *ROP* is much-needed to guarantee the success and profitability of those drilling applications.

Drilling engineering is a multidisciplinary area in which several science branches, including geology, petroleum engineering, mechanical engineering, metallurgy engineering, electronics, robotics, computer engineering, etc., come together to make drilling operations more energy-efficient, affordable, and time-efficient [58]. The objective of this research is to integrate the previous and recent advancements in *ROP* prediction for recognition of current limitations and future requirements pertinent to different aspects of *ROP* modeling. Therefore, in this study, from miscellaneous angles including the contributing factors, types (empirical and AI-based) of models, and potential shortcomings, *ROP* models are assessed.

The current research reveals that uncontrollable factors have not been adequately incorporated into the existing *ROP* models. To address this issue, four uncontrollable factors, including rock permeability, wellbore inclination, temperature, and rock hardness, are suggested to be added to future *ROP* models. The novelty of the current research lies in the detection of such uncontrollable factors to improve *ROP* models. To find the relation between those factors and *ROP* variation, both laboratory tests and AI approaches can be utilized. Moreover, since the uncontrollable factors mostly originated from uncertainty in the geological properties of the subsurface formations, development of a formation-based classification system of input parameters is proposed. For instance, the rock abrasiveness can be applied in sandstone *ROP* models, not for salt rocks. On the contrary, the rock creep can be included in salt rocks *ROP* models, not for sandstone rocks. Through this, for different formations, the minimum number of effective geological parameters can be included in *ROP* models.

The structure of this research has been designed as follows: in Section 2, the different contributing factors in *ROP* modeling are described. Then, in Section 3.1, the different empirical *ROP* models are elaborated and compared with each other. Afterwards, in Section 3.2, the focus shifts to AI-based studies performed for *ROP* prediction/optimization. In that section, the type of input data, the merits, and demerits of those AI-based models are also described and contrasted. Then, in Section 4, an inclusive discussion on the key results and recognized shortcomings is presented. Finally, the article ends with a concise conclusion depicting the main results, propositions, and implications of this research.

2. Contributing Factors on the ROP

To enhance and develop *ROP* models, it is necessary to investigate the factors affecting this parameter. The most important contributing factors on the *ROP* can be divided into two main groups: uncontrollable and controllable factors [33]. Figure 1 depicts these factors. The main uncontrollable factors stem from the uncertainty in the formation characteristics. No adequate attention has been given to these factors in available *ROP* models for oil/gas drilling operations. However, in the mining industry, it seems that researchers have incorporated more physical and mechanical properties of formations into *ROP* models. On the opposite side, the number of controllable factors affecting the *ROP* are more than the uncontrollable ones. Therefore, in the real field, the controllable factors are usually changed to enhance the *ROP*. The main controllable factors included in the available oil/gas *ROP* models are "rig operating conditions", "drilling fluid properties", and "bit hydraulics". In the mining industry, less investigation has been dedicated to the parameters of rig operating conditions, including the *WOB*, *RPM*, bit type, and torque. Those factors are elaborated in what follows.

2.1. Formation Characteristics

There are several formation characteristics influencing the bit-penetration rate. One of the most determining characteristics is the shear strength of the rock. For a standard compression test, the following formula can be utilized to calculate the rock shear strength [59]:

$$\tau_0 = \frac{\sigma_1}{2}\cos\theta \tag{1}$$

where τ_0 (psi) represents the rock shear strength, σ_1 (psi)represents the rock compressive strength, and θ depicts the internal friction angle. There are several rock-failure criteria to predict the rock shear strength. Some examples are the Hoek–Brown, Drucker–Prager, Mohr–Coulomb, and Modified Lade. Those criteria are based on some assumptions which may affect the predicted value of the shear strength of the rock.

Moreover, the elemental composition of rocks has an impact on the *ROP* values. For example, rocks containing a high percentage of hard minerals, e.g., SiO_2 and Fe_2O_3, have less drillability in comparison to the rocks containing clay minerals. Abrasiveness is another important factor affecting the *ROP*. For instance, the common igneous rocks, such as granite and diorite, are more abrasive than the sedimentary formations, such as sandstone and shale. Such high abrasiveness gives rise to a premature, fast dulling of the bit's teeth [59].

Rock permeability is another parameter that has a remarkable influence on the *ROP*. In fact, permeability allows the drilling fluid to move into the subsurface layers, thereby equalizing the pressure differential at the bottom-hole.

Poroelastic properties of rocks also play a significant role in the interaction between the rock and the bit, thereby affecting the *ROP* [60]. Such poroelastic properties are derived from the presence of pore pressure within the pores of rocks. The main poroelastic parameters include the porosity, pore pressure, Biot's coefficient, and Skempton's coefficient [61]. During the drilling operations, the coupling between the pore pressure, mud flow, *WOB*, and the in situ stresses cause deformations around the wellbore. Such coupling is of paramount significance in terms of wellbore instability problems [62], lost circulation issues, wellbore deviation from the planned trajectory, etc. It should be noted that the poroelastic parameters are dependent on the temperature of the surrounding formations [63,64].

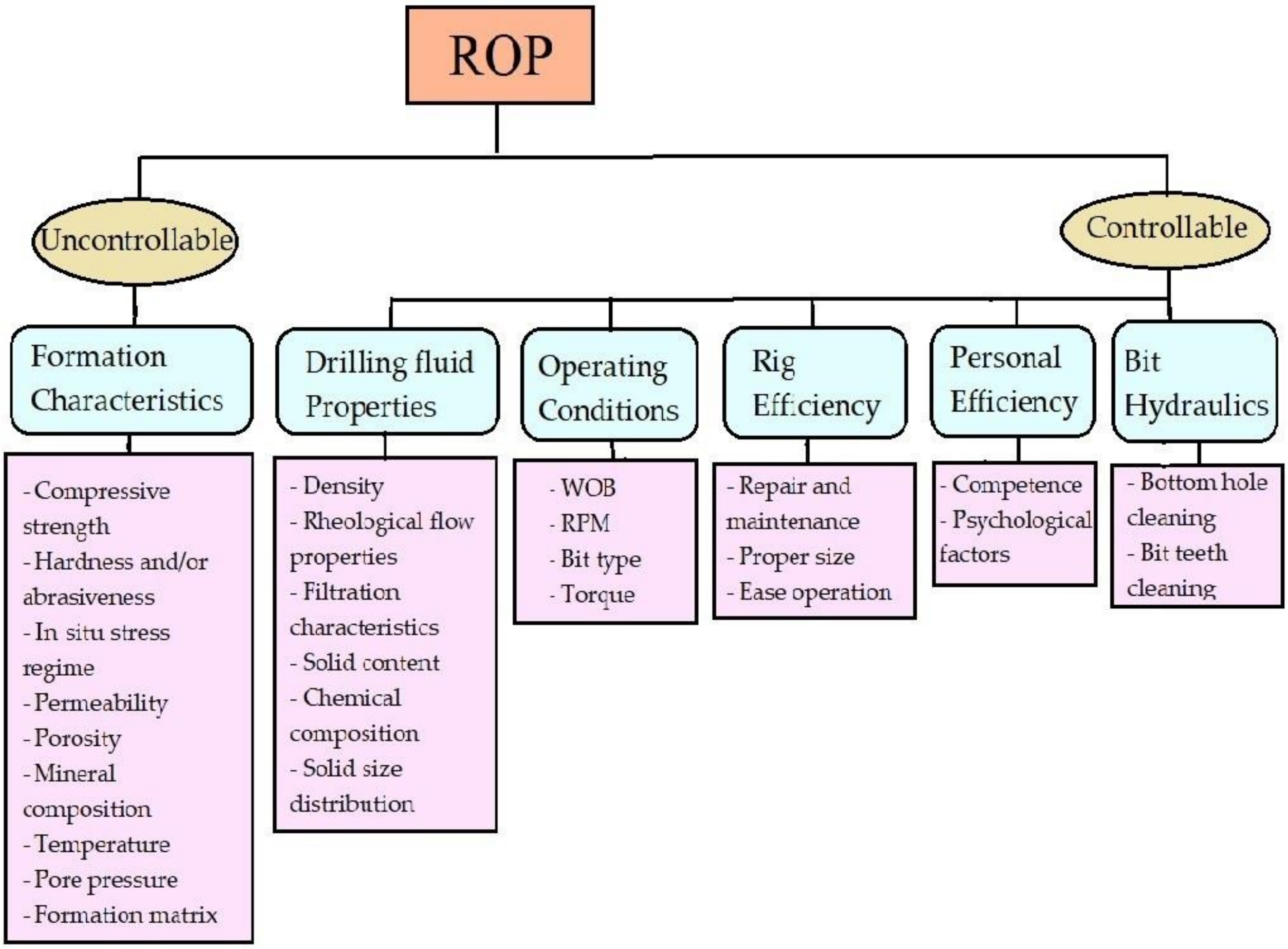

Figure 1. The summary of contributing factors on the *ROP*.

2.2. Mud Properties

Muds play an integral role in every drilling operation. Some vital functions of mud include the cuttings removal, prevention of pore fluid influx into the wellbore, and preservation of the wellbore stability. Therefore, providing an accurate drilling fluid system is quite crucial for successful drilling. To appropriately characterize the drilling fluid, calculation of the fluid flow and its pressure within the wellbore is of paramount significance. The science of wellbore fluid mechanics is applied to investigate the influence of mud characteristics on the drilling operations. In other words, wellbore fluid mechanics describes the dominant equations on the fluid flows in the wellbore to predict their performance during the interaction with the surrounding formations, and pore fluids at different depth and temperature conditions.

Regarding the mud, the chemical composition, viscosity, density, and solid content of the mud are of paramount significance. For instance, when it comes to the chemical composition, water-based drilling fluids may interact with shale formations, thereby gradually washing them. Consequently, such circumstances may bring about wellbore instability issues. Concerning mud viscosity, it is a critically important fluid characteristic in the *ROP* optimization. The mud viscosity is a determining factor in the cleaning and transportation of the rock cuttings towards the ground surface.

Furthermore, the solid content along with the mud density regulate the differential pressure in the bottom-hole. Drilling fluids with high density create a positive differential pressure around the bit (overbalanced drilling). The correlation between the overbalanced drilling and the *ROP* for different bit types has been shown in Figure 2. As it can be seen, such correlation is a straight line when the values of log (R/R_0) are presented as a function of the overbalance pressure. The parameters of R and R_0 represent the *ROP* and the initial *ROP*, respectively. On the other hand, when the mud density is less than the formation pressure, underbalanced drilling occurs. Based on this figure, when drilling is performed under underbalanced conditions, the *ROP* values increase [59].

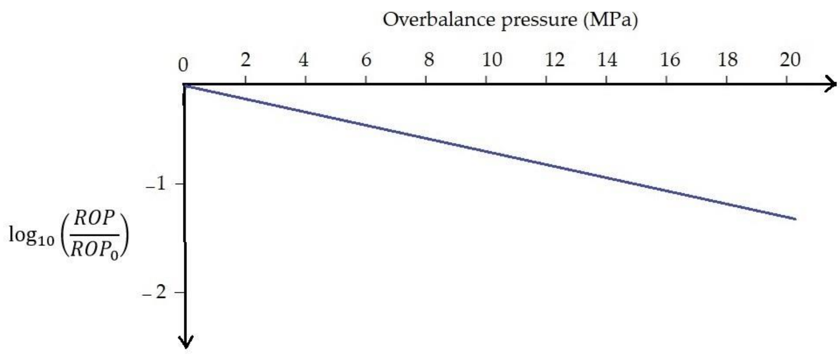

Figure 2. The variation of the *ROP* with overbalance pressure.

Bourgoyne and Young offered the following relation between the overpressure (overbalance) and the *ROP* (ft/h) [3]:

$$\log_{10}\left(\frac{ROP}{ROP_0}\right) = -m\left(P_{bh} - P_f\right) \tag{2}$$

where P_{bh} (psi) demonstrates the circulating bottomhole pressure P_f (psi) depicts the pore fluid pressure ROP_0 (ft/h) is the *ROP* at zero overbalance, and m is the tangent of the straight line in Figure 2. The parameter of P_{bh} can be calculated as:

$$P_{bh} = 0.052\rho_c D \tag{3}$$

where ρ_c (Ib/gal) represents the ECD, and D (ft) is the total depth. Moreover, the pore fluid pressure is calculated as:

$$P_f = 0.052 g_p D \tag{4}$$

where g_p (Ib/gal) represents the gradient pore pressure. Equations (2) and (4) can be rewritten as:

$$\log_{10}\left(\frac{ROP}{ROP_0}\right) = -0.052 m D\left(\rho_c - g_p\right) \tag{5}$$

$$\log_{10}\left(\frac{ROP}{ROP_0}\right) = -a_4 D(\rho_c - g_p) \tag{6}$$

where a_4 is the overbalance exponent. The above-mentioned equations are beneficial to investigate the influence of the mud density on the *ROP*. Thus, Equation (6) is rewritten as:

$$\frac{ROP_2}{ROP_1} = e^{2.304 a_4 D(\rho_1 - \rho_2)} \tag{7}$$

where, ROP_1 and ROP_2 represent the *ROP* values related to the ρ_1 and ρ_2 respectively. Note that ρ_1 (Ib/gal) is the initial mud weight while ρ_2 (Ib/gal) is the secondary one [3].

2.3. Bit Operating Conditions

The parameters pertinent to the bit working conditions also affect the *ROP* values. Such parameters include the bit type, bit tooth wear, *RPM*, *WOB*, and torque.

Regarding the bit wear, it is noticeable that, due to the tooth wear, most bits drill more slowly as drilling time passes. Abrasion and chipping mechanisms decrease the tooth length continuously. Hard facing erodes the tooth in a way that encourages self-sharpening tooth wear. Although such action maintains the tooth sharpness, the shorter tooth length is not compensated by this. The tooth of PDC bits and rolling-cutter bits constructed of tungsten carbide fail via breaking rather than abrasion [2,15,65–67].

Another important factor in *ROP* optimization is the torque. It is stated that torque becomes significantly more sensitive to the variations of *WOB* as the bit penetrates further into the deeper hard rocks [68].

Regarding the *RPM*, Figure 3 illustrates the relation between the *RPM* and the *ROP* (red curve). For the low values of *RPM* (segment ab), there is a direct, linear relationship between the *RPM* and the *ROP*. The green dashed line illustrates such linear relation. Point b is known as the foundering point. After point b, the rise in the *RPM* causes a nonlinear increase in the *ROP* with a slower pace (segment bc). Such reduction is due to the inefficient bottom-hole cleaning and mud characteristics, such as buoyancy factor [59].

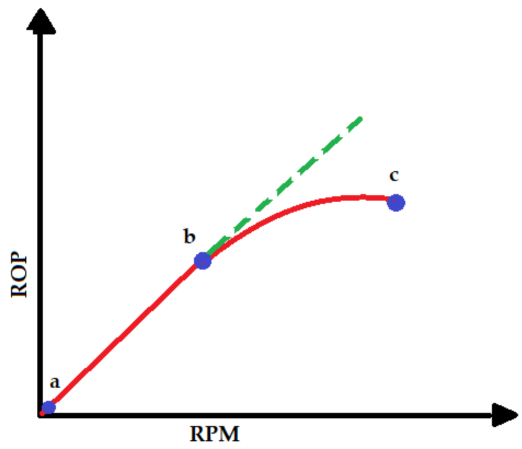

Figure 3. Variation of the *ROP* as a function of *RPM*.

Regarding the *WOB*, Figure 4 depicts the change of the *ROP* versus the *WOB* (red curve). Note that no tooth wear is assumed in this figure. Point a is known as the threshold formation stress. Before point a is surpassed, no substantial penetration rate is obtained. For the low values of bit weight (segment ab), the *ROP* builds up linearly with rising values. The moment at which the rock-failure condition switches from scraping to shearing is known as point b. After point b, as the *WOB* increases, the *ROP* heightens linearly (segment bc); however, this segment has a steeper slope than the segment ab, thereby indicating a higher drilling efficiency. Beyond point c, additional bit weight enhances the *ROP* marginally (segment cd). Point d is the foundering point. After point d, in some instances, the *ROP* drops off at excessively large *WOB* values (segment de). The reason is that for the intensely high *WOB*s, the bottom-hole cleaning and cutting removal mechanisms become inefficient due to the large volume of rock cuttings produced in the bottom-hole. Such a situation also prevents the mud from escaping from the nuzzles, thereby leading to further inefficient bottom-hole cleaning [37,59].

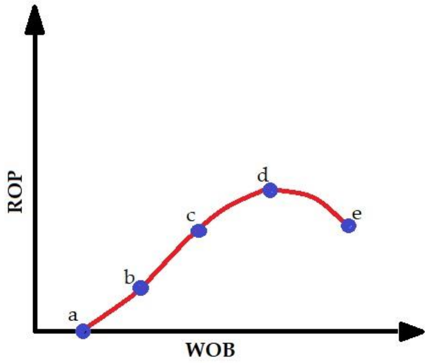

Figure 4. Variation of the *ROP* vs. *WOB*.

2.4. Bit Hydraulics

Optimization of bit hydraulics for acquisition of high *ROP* values has been the subject of much debate [69,70]. Commonly, the mentioned factors include the Reynolds number, mud-flow rate, impact force of the jet, nuzzle velocity, and bit hydraulic horsepower. Many researchers believe that the bit's foundering point is affected by the hydraulic pressure attained at the bit. Eckel proposed the underlying relation based on the Reynolds number [18]:

$$N_{R_e} = K_s \frac{\rho_f Q d_{nz}}{\mu_a} \tag{8}$$

where N_{Re} stands for the Reynolds number function, K_s represents the scaling coefficient, ρ_f (Ib/gal) indicates the density of mud, Q (gal/min) represents the fluid-flow rate, d_{nz} (in) indicates the diameter of nozzle, and μ_a (cp)) represents the mud's apparent viscosity at $10^4\ s^{-1}$. Figure 5 displays the impact of the Reynolds number function and *WOB* on the *ROP* [18]. For the whole range of the Reynolds numbers investigated, the penetration rate rises as the Reynolds number function increases. As it can be observed, the corresponding curve moves upward as the *WOB* is raised. It is noteworthy that Eckle did not investigate the effect of the foundering point on the *ROP*.

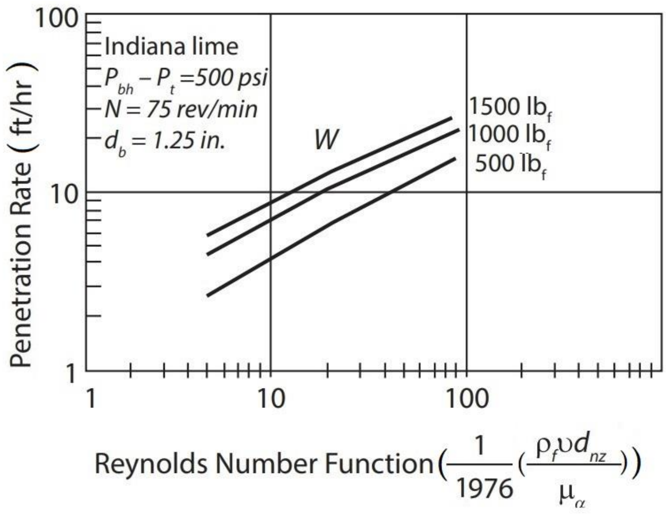

Figure 5. The impact of the Reynolds number function and *WOB* on the *ROP* [18].

2.5. Personal Efficiency

Any drilling issue can result in extremely high overall well expenses; as a result, ongoing training for all drilling crew is crucial to achieve high *ROP* values [37,71].

2.6. Rig Efficiency

Selection of a proper rig for the drilling operation is of paramount importance. The selected rig can influence the whole drilling cost, time, and specified energy. Moreover, appropriate maintenance is required to keep the rig in an operable condition. The simplicity of the rig is also beneficial for the crew to take correct, rapid actions during the drilling operation.

3. The ROP Models

A number of empirical and data-driven models have been established to predict or optimize the *ROP*. The empirical models were mainly developed using real field drilling data or laboratory tests. The linear regression technique was mostly used to formulate the *ROP* relationship with other drilling parameters. On the opposite side, the data-driven models forecast the *ROP* values using AI techniques [72]. Both types of *ROP* models are elaborated in what follows.

3.1. Empirical ROP Models

3.1.1. Review on Empirical ROP Models

Maurer created the first empirical model for *ROP* prediction [14]. The main components of that model were the rock strength, *WOB*, *RPM*, and drill bit diameter. The following equation describes Maurer's model:

$$ROP = \frac{K}{S^2}\left(\frac{WOB}{d_{bit}} - \frac{WOB_0}{d_{bit}}\right)^2 RPM \tag{9}$$

In this equation, K shows the proportionality coefficient, WOB (Ib) represents the weight on the bit, d_{bit} (in) demonstrates the bit diameter, RPM (rev/min) is the rotational speed of the bit, WOB_0 (Ib) depicts the threshold weight on the bit, and S represents the rock compressive strength.

Galle and Woods proposed the second *ROP* model [15]. The corresponding formula was:

$$ROP \propto \left(\frac{1}{0,\ 928125{h_f}^2 + 6h_f + 1}\right)^{b_7} \tag{10}$$

In this equation, h_f (in) depicts the fractional bit tooth dullness, and b_7 shows an exponent (suggested to be selected as 0.5).

Bingham proposed a different model to forecast the *ROP* [16]. The model was expressed as:

$$ROP = K\left(\frac{WOB}{d_{bit}}\right)^{b_5} RPM \tag{11}$$

where b_5 is the WOB exponent. In addition, K included the rock strength from Maurer's model.

One of the most practical empirical models to forecast the *ROP* was developed by Bourgoyne and Young [3]. This *ROP* model was defined by the following equation:

$$ROP = f_1 \times f_2 \times f_3 \times f_4 \times f_5 \times f_6 \times f_7 \times f_8 \tag{12}$$

where

$$f_1 = exp^{2.303 \times a_1} \tag{13}$$

$$f_2 = exp^{2.303 \times a_2 \times (10000 - TVD)} \tag{14}$$

$$f_3 = exp^{2.303\times a_3 \times TVD^{0.69}\times(g_p-9.0)} \tag{15}$$

$$f_4 = exp^{2.303\times a_4 \times TVD\times(g_p-ECD)} \tag{16}$$

$$f_5 = \left[\frac{\left(\frac{WOB}{d_{bit}}\right) - \left(\frac{WOB}{d_{bit}}\right)_t}{4 - \left(\frac{WOB}{d_{bit}}\right)_t}\right]^{a_5} \tag{17}$$

$$f_6 = \left(\frac{RPM}{60}\right)^{a_6} \tag{18}$$

$$f_7 = exp^{-a7\times h_f} \tag{19}$$

$$f_8 = \left(\frac{F_{Jet}}{1000}\right)^{a_8} \tag{20}$$

In Equations (12)–(20), a_1, a_2, a_3 ... , and a_8 are determined using real drilling data. Moreover, TVD (ft) displays true vertical depth, g_p (Ib/gal) indicates the gradient of pore fluid pressure, $(WOB/d_{bit})_t$ stands for the parameter of the threshold *WOB* pertinent to one inch of the bit diameter when the bit starts drilling (10^3 lbf/in), F_{Jet} (Ib) demonstrates the fluid motion force beneath the bit, and (WOB/d_{bit}) represents the *WOB* pertinent to one inch of bit diameter. It is also important to note that Osgouei enhanced this model in 2007 by adding the hole-cleaning term for directional and horizontal wellbores [68]. Such an improved model is applicable for both roller-cone bits and PDC bits [68].

Furthermore, the parameter of bit wear was presented by utilization of some specific assumptions. The tooth wear can be calculated as [3]:

$$\frac{dh}{dt} = \frac{H_3}{\tau_H}\left[\frac{RPM}{100}\right]^{H_1} \times \left\{\frac{\left(\frac{WOB}{d_{bit}}\right)_{max} - 4}{\left(\frac{WOB}{d_{bit}}\right)_{max} - \frac{WOB}{d_{bit}}}\right\} \times \left\{\frac{1+\frac{H_2}{2}}{1+H_2 h}\right\} \tag{21}$$

where h (ft) is the depth and t (h) is time. The coefficients of H_1, H_2, and H_3 are dependent on the type of bit. Moreover, τ_H is a coefficient representing the abrasiveness of the rock. To calculate the bearing wear, the following relationship was proposed:

$$\frac{dB_{bw}}{dt} = \frac{1}{\tau_b} \times \frac{RPM}{100} \times \left[\frac{WOB}{4d_{bit}}\right]^b \tag{22}$$

where B_{bw} is the bearing wear proportion over the bearing's entire lifetime, τ_b (h) is the lifetime of the tooth under standard circumstances, and b is an empirical coefficient.

Reza and Alcocer in Ref. [66], used the Buckingham p-theorem to express a nonlinear drilling model for deep-drilling operations. In their model, the *ROP* was expressed through the following equation:

$$\frac{ROP}{RPMd_{bd}} = K\left[\frac{RPMd_{bd}^2}{v}\right]^a\left[\frac{RPMd_{bd}^3}{Q}\right]^b\left[\frac{Ed_{bd}}{WOB}\right]^c\left[\frac{\Delta pd_{bd}}{WOB}\right]^d \tag{23}$$

where K shows the proportionality constant, d_{bd} (in) represents the diameter of bearing, v (cp) represents the kinematic viscosity of the mud, Q (gal/min) demonstrates the mud-flow rate, Δp (psi) is the differential pressure between the mud pressure and pore pressure, and E (psi) represents the formation hardness. It is noteworthy that the variables of K, a, b, c, and d were calculated using regression analysis. Finally, the following *ROP* equation was obtained:

$$\frac{ROP}{RPMd_{bd}} = 0.33\left[\frac{RPMd_{bd}^2}{v}\right]^{-0.43}\left[\frac{RPMd_{bd}^3}{Q}\right]^{-0.68}\left[\frac{Ed_{bd}}{WOB}\right]^{-0.91}\left[\frac{\Delta pd_{bd}}{WOB}\right]^{-0.15} \tag{24}$$

In addition, the general relationship for calculation of bit dulling was proposed as:

$$\frac{h_f}{RPMd_{bit}} = 0.001[\frac{Q}{RPMd_{bit}{}^3}]^{0.56}[\frac{WOB}{Ed_{bit}{}^2}]^{0.26}[\frac{d_{bit}}{Q}]^{-0.03} \quad (25)$$

where h_f is the fractional dullness of the bit tooth. On the other side, the general relationship for bit-bearing life was expressed as:

$$\frac{B_{bw}}{RPM} = 0.05[\frac{Th_t d_{bd}}{RPM\ WOB}]^{0.51}[\frac{v}{RPMd_{bd}{}^2}]^{0.26}[\frac{Q}{RPMd_{bd}{}^3}]^{-0.5} \quad (26)$$

where T (°F) is the temperature of the bottom-hole setting and h_t (Btu/°F) is the coefficient of heat transfer.

The "perfect-cleaning model" was proposed by Warren [20]. The model had variables of bit diameter, rock strength, RPM, and WOB. The corresponding formula was:

$$ROP = 1/(\frac{aS^2 d_{bit}^3}{RPM^b WOB^2} + \frac{b}{RPMd_{bit}}) \quad (27)$$

where a and b represent two dimensionless coefficients and S (psi) represents the rock's strength. The applicability of this model was constrained as it did not consider the cuttings removal. To address this issue, Warren proposed the "imperfect-cleaning model". The improved model included the cuttings removal which is influenced by the density and viscosity of the mud, as well as the impact force of the jet. Consequently, this model became more applicable than the former one. The model is represented by the following equation:

$$ROP = 1/(\frac{aS^2 d_{bit}^3}{RPM^b WOB^2} + \frac{b}{RPMd_{bit}} + \frac{cd_{bit}\gamma_f \mu}{F_{jet}}) \quad (28)$$

where c is a dimensionless constant, γ_f stands for the fluid-specific gravity, and μ (cp) indicates the viscosity of the drilling fluid. Moreover, F_{jet} (Ib) shows the impact of the jet force.

Warren's imperfect-cleaning model was modified by Hareland and Rampersad [24]. They incorporated the impact of bit wear in the above equation by proposing a wear function, W_f, as:

$$ROP = W_f/[f_c(P_e)\left(\frac{aS^2 d_{bit}^3}{RPM^b WOB^2} + \frac{b}{RPMd_{bit}} + \frac{cd_{bit}\rho_f \mu}{F_{jet}}\right)] \quad (29)$$

$$W_f = 1 - \frac{\Delta BG}{8} \quad (30)$$

where a, b, and c are dimensionless constants, $f_c(P_e)$ represents the chip hold-down function, and ΔBG is the variation of the bit-tooth wear. The parameter of ΔBG is obtained through:

$$\Delta BG = W_c[\sum_{i=1}^{n} WOB_i RPM_i S_i (A_{r_{abr}})_i] \quad (31)$$

where W_c represents the bit-wear constant. Moreover, $A_{r_{abr}}$ indicates rock relative abrasiveness and S (psi) represents the rock confined compressive strength obtained through the following relationship:

$$S = S_0[1 + a_s\ P_e{}^{b_s}] \quad (32)$$

where S_0 (psi) represents the unconfined strength of rock. In addition, the constants of a_s and b_s (md) are dependent on the rock permeability.

Osgouei suggested the final prominent empirical model, in Ref. [68]. The Bourgoyne and Young model served as the foundation of his model. Osgouei added three factors, specifically, f_9, f_{10}, and f_{11}, which represent the borehole cleaning terms in the horizontal, directional, and vertical wellbores for both the roller-cone and the PDC bits. In fact, he accounted for the impact of the hole-cleaning factor on the values of the *ROP*. The *ROP* model improved by Osgouei is:

$$ROP = f_1 \times f_2 \times f_3 \times f_4 \times f_5 \times f_6 \times f_7 \times f_8 \times f_9 \times f_{10} \quad (33)$$

where

$$f_1 = e^{a_1} \quad (34)$$

$$f_2 = e^{a_2 \times (8800 - TVD)} \quad (35)$$

$$f_3 = e^{a_3 \times TVD^{0.69} \times (g_p - 9)} \quad (36)$$

$$f_4 = e^{a_4 \times TVD \times (g_p - ECD)} \quad (37)$$

$$f_5 = \left[\frac{\frac{WOB}{d_{bit}}}{\left.\frac{WOB}{d_{bit}}\right|_t} \right]^{a_5} \quad (38)$$

$$f_6 = \left(\frac{RPM}{RPM_c} \right)^{a_6} \quad (39)$$

$$f_7 = e^{-a7\ h_f} \quad (40)$$

$$f_8 = \left(\frac{F_{Jet}}{F_{Jc}} \right)^{a_8} \quad (41)$$

$$f_9 = \left(\frac{A_{bed}/A_{well}}{0.2} \right)^{a_9} \quad (42)$$

$$f_{10} = \left(\frac{V_{Actual}}{V_{Critical}} \right)^{a_{10}} \quad (43)$$

$$f_{11} = \left(\frac{C_c}{100} \right)^{a_{11}} \quad (44)$$

The constants of a_1, a_2, $_3$, ..., and a_{11} are estimated through real drilling data. Moreover, RPM_c (rev/min) stands for the critical rotary speed, which must be estimated by considering the characteristics of the drilling string, bit type, and field data. Additionally, the parameter of F_{Jc} is dependent on the type of bit, the mud's characteristics, and pump pressure. In addition, h_f displays the fractional tooth dullness. The parameter of V_{Actual} (ft/s) denotes the volume of clippings, $V^{critical}$ (ft/s) is the critical volume of the cuttings removal, and C_c is the constant of the cuttings concentration. The parameters of A_{bed} (ft^2) and A_{well}(ft^2) demonstrate the area of the cuttings bed and the wellbore, respectively.

3.1.2. Analysis of the Empirical ROP Models

The most well-known empirical *ROP* models were elaborated in the previous section. As mentioned, different researchers had strived to improve *ROP* models by adding new contributing factors to them. This is why empirical *ROP* models underwent continuous improvements from the early Maurer model to Osgouei's model. Table 1 summarizes the different controllable and uncontrollable factors applied in those empirical *ROP* models. Based on Table 1, the total frequency of those controllable and uncontrollable factors was calculated (Figure 6). Furthermore, the frequency of each individual factor in *ROP* models was quantified. The results are depicted in Figure 7.

Table 1. Factors considered in existing empirical *ROP* models.

Reference	Controllable Factors											Uncontrollable Factors							
	WOB	*RPM*	d_{bit}	h_f	F_{Jet}	TVD	μ	B	ρ_f	Q	P_m	S	Ab	E	P_p	T	*Pe*	C_c	A_{well}
Maurer, 1962 [14]	×	×	×									×							
Galle and Woods, 1963 [15]				×															
Bingham, 1965 [16]	×	×	×									×							
Bourgoyne and Young, 1974 [3]	×	×	×	×	×	×		×	×		×	×	×		×				
Warren (perfect model), 1981 [6]	×	×	×									×							
Warren (imperfect model), 1984 [7]	×	×	×		×		×		×			×							
Reza and Alcocer, 1986 [64]	×	×		×			×	×		×	×			×	×	×			
Hareland and Rampersad, 1994 [24]	×	×	×	×	×		×		×			×	×				×		
Osgouei, 2007 [5]	×	×	×	×	×	×	×	×	×		×	×	×		×			×	×

WOB: weight on the bit, *RPM*: rotational speed, d_{bi}: diameter of bit, h_f: bit-tooth wear, F_{Jet}: fluid motion force beneath the bit, TVD: true vertical depth, μ: mud viscosity, B: bearing wear, ρ_f: mud density, Q: flow rate, P_m: mud pressure, S: rock strength, Ab: rock abrasiveness, E: rock hardness, P_p: pore pressure, T: temperature, *Pe*: rock permeability, C_C: cutting properties, A_{well}: wellbore cross-sectional area.

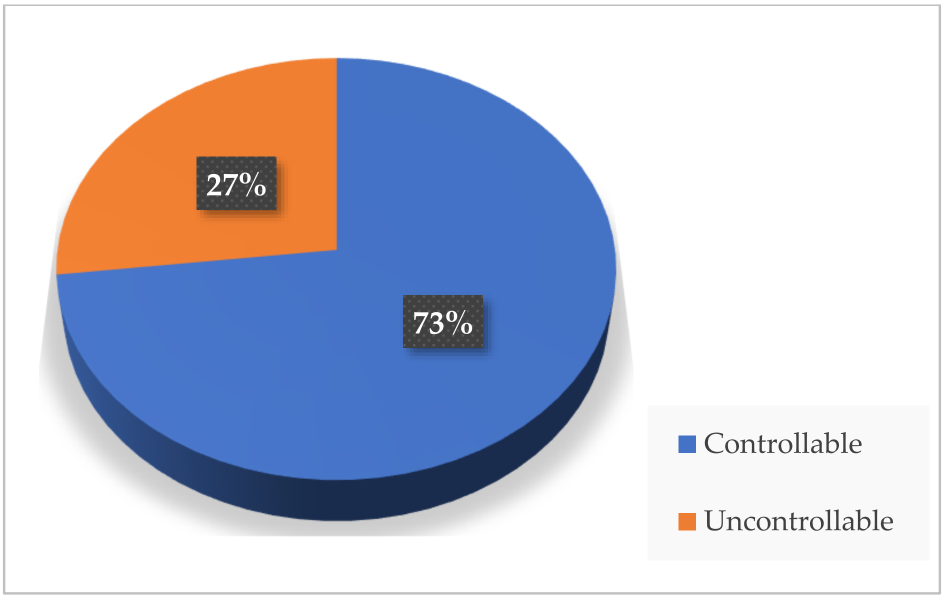

Figure 6. The percentage of controllable and uncontrollable factors in empirical *ROP* models.

Based on Figure 6, only 27% of the investigated factors belong to the uncontrollable category. Hence, in comparison to the controllable factors, the uncontrollable factors are required to be further included in future *ROP* models.

In addition, according to Figure 7, it can be seen that *WOB* and *RPM* are the controllable factors with highest frequency. Furthermore, rock strength (*S*) is the most frequent uncontrollable factor applied in the models. By contrast, flow rate (*Q*), rock hardness (E), cutting properties (*Cc*), temperature (T), and permeability (*Pe*) are the parameters with the least repetition in the models. Amongst these parameters, only the flow rate is controllable while the rest are uncontrollable factors. Thus, the influence of these low-frequent parameters needs to be further investigated in future studies.

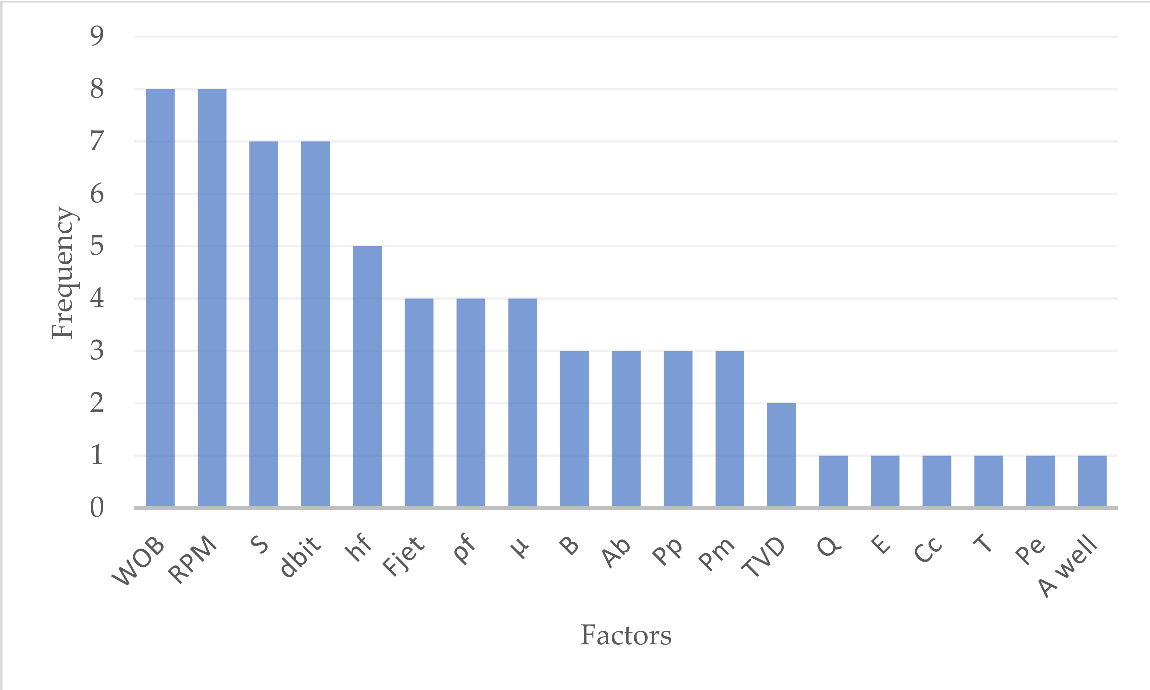

Figure 7. The frequency of different factors used in empirical *ROP* models.

Apart from the contributing factors, the applicability of each *ROP* model is also of paramount importance. Such applicability can be considered from the perspectives of bit type and wellbore direction.

In drilling engineering, bits are commonly divided into two main groups: roller-cone bits and fixed-cutter bits. Figure 8 illustrates those types of bits. The *ROP* can be remarkably affected by the type of bit. For instance, the initial *ROP* of roller-cone bits is commonly the highest, especially for bits with large offset and long teeth. These kinds of bits are suitable for soft formations since the *ROP* decreases after the bit penetrates deeper rocks, especially into the harder layers [37]. On the contrary, the fixed-cutter bits destroy the rocks through a wedging-type fragmentation mechanism. Thus, the bottom-cutting angle and number of blades have predominant effects on the *ROP* per each revolution.

The second applicability is wellbore direction. In the past, most of the wellbores were drilled vertically; however, due to the emergence of new technologies, such as hydraulic fracturing, the drilling companies tend to drill wellbores directionally. Such directional wellbores access more hydrocarbon-bearing formations, thereby allowing the companies to increase total oil and gas production. For instance, from 2010 to 2021, as a consequence of widespread directional drilling in the US, the total number of completed wellbores decreased by 66%, and average drilling length declined by 30%; however, the production of crude oil increased by two times [73]. In 2021, only 19% of US wellbores were drilled vertically, while 81% of the wellbores had directional trajectories.

Table 2 demonstrates the applicability of different *ROP* models in terms of bit type and wellbore direction. According to this table, the majority of empirical *ROP* models have been developed for roller-cone bits. Moreover, only two models, specifically, Reza and Alcocer's model and Osgouei's model, can be applied for roller-cone bits and fixed-cutter bits. Regarding the wellbore direction, only Osgouei's model is applicable for both vertical and directional wells. Therefore, any future investigation must consider the applicability of the proposed *ROP* models for directional wellbores.

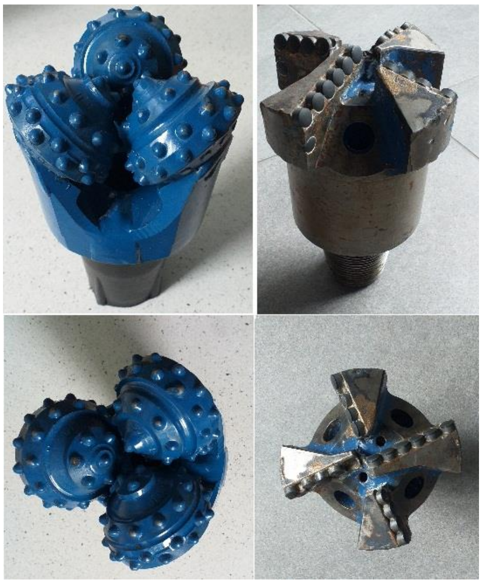

Figure 8. Different bit types: fixed-cutter bit (**right**), and roller-cone bit (**left**) [59].

Table 2. Applicability of empirical *ROP* models in terms of bit type and well direction.

Reference	Bit Type		Well Direction	
	Roller-Cone Bit	**Fixed-Cutter Bit**	**Vertical**	**Directional**
Maurer, 1962 [14]	×		×	
Galle and Woods, 1963 [15]	×		×	
Bingham, 1965 [16]		×	×	
Bourgoyne and Young, 1974 [3]	×		×	
Warren (perfect model), 1981 [6]	×		×	
Warren (imperfect model), 1984 [7]	×		×	
Reza and Alcocer, 1986 [64]	×	×	×	
Hareland and Rampersad, 1994 [24]		×	×	
Osgouei, 2007 [5]	×	×	×	×

3.1.3. Shortcomings and Limitations of Existing Empirical ROP Models

In the previous sections, different empirical *ROP* models, together with their required factors, were elaborated. Moreover, the frequency of each influential factor in existing *ROP* models was quantified (Figure 7). As mentioned earlier, four uncontrollable factors, specifically, rock permeability (*Pe*), temperature (T), cuttings concentration coefficient (*Cc*), and hardness (E), have not been sufficiently incorporated into the *ROP* models. Hence, in the current section, a brief debate is given to clarify why and how those factors can be deployed to improve future *ROP* models:

- Rock permeability represents the capacity of rock to allow fluid to move through the rock pores. In nature, such fluid is water, brine, oil, etc. During drilling operations, the bit cutters break the rock, and, simultaneously, the mud pressure prevents the pore fluid from flowing into the well space. In a microscopic perspective, the bit pushes the pore fluid back through two mechanisms [74]. In the first mechanism, the mud pushes back the pore fluid directly, thereby driving it to flow backwards. This mechanism is dominantly governed by the bit-rotation speed. In the second mechanism, the pores are compressed by bit cutters, and, consequently, the pore fluid is squeezed away from the bottom hole. This mechanism is mainly governed by rock diffusivity which is directly related to the rock permeability. Therefore, since the rock permeability changes, the *ROP* is altered [74]. Thus, it is suggested that more investigations on the relations between rock permeability and the *ROP* are conducted to improve the previous empirical models or to develop new ones;

- The second less-frequent factor is the coefficient of cuttings concentration which can be utilized as an indicator of the cuttings volume accumulated at the bottom hole. This factor is especially determining in the *ROP* during drilling of directional wells. As mentioned in the previous section, with the increasing demands for production from unconventional reservoirs, directional (horizontal and inclined) drilling has markedly increased; however, some features of past *ROP* models were considered only for vertical wells. Thus, it is essential to account for those features in *ROP* models developed for directional wellbores. The coefficient of cuttings concentration is such an essential factor.

During the drilling of directional wells, cuttings may be excessively deposited on the lower side of the wellbore. This leads to formidable changes, such as reduced weight transmitted to the bit, and intense friction between the drill pipe and wellbore wall. To consider this effect, the *WOB* must be modified in *ROP* models. For this purpose, the following formula is suggested [75]:

$$WOB_d = WOB_s \times e^{-\mu \times \theta} \tag{45}$$

where WOB_d (Ib) represents the modified *WOB* for directional drilling, μ indicates the coefficient of sliding friction, WOB_s (Ib) is the measured *WOB* at the surface, and θ (radian) is the wellbore inclination angle. Generally, the WOB_d is less than the WOB_s. If this difference is not applied for the *ROP* models developed for directional drilling, the accuracy of the model may decline to a great extent.

- The third parameter is rock hardness. Rock hardness can be defined as the rock resistance to drilling. In other words, rock hardness is reciprocal of drillability. Some researchers have linked hardness with drilling speed; other researchers related the hardness to the amount of energy required for cutting a unit volume of rock [76]. Rock hardness is mainly dependent on the hardness of the minerals, grain size, grain shape, grain distribution, and cementation material. The silica content of the rock greatly affects the rock hardness. Although other resistive features, such as compressive strength and rock abrasiveness, have been adopted more frequently in *ROP* models, the inclusion of rock hardness into *ROP* models seems to be necessary;
- Temperature is another factor influencing the penetration rate. The bit brecks the rock under a thermo–hydro–mechanical condition. During the drilling operation, the bit penetrates the deeper formations with different thermal conditions. The heat changes the poroelastic properties of the rocks as well as the characteristics of the pore fluid [63,64]. One of those important poroelastic parameters is Biot's coefficient. When the temperature changes, Biot's coefficient varies and has an impact on the effective stress applied on the rock at the bottom hole. As a matter of consequence, the rock compression or shear strength changes, thereby influencing the *ROP*. Hence, the impact of temperature should be regarded in *ROP* models, especially using inclusion of Biot's coefficient as a temperature-dependent factor.

3.2. Data-Driven ROP Models

Empirical *ROP* models may deliver inaccurate results since they cannot take into account all contributing factors [77–82]. Therefore, a number of researchers made efforts to deploy AI techniques in *ROP* modeling works [83,84]. During drilling operations, a significant amount of data is gathered daily. Because of this, some petroleum engineers and researchers turned to AI methods to forecast the *ROP*. The AI algorithms allowed the engineers to thoroughly evaluate the gathered data and produce valuable insights. Such AI techniques are used in a variety of applications related to drilling issues [85–91].

So far, several AI approaches have been utilized in *ROP* modeling. Table 3 summarizes the outstanding data-driven *ROP* models established by different researchers. As it can be seen, the majority of those studies have applied the ANN approach. Moreover, a wide spectrum of input parameters has been deployed in AI-based models.

ANNs resemble how the brain uses its biological neurons to process information to learn features [92,93]. Every ANN model possesses at least three structural layers: input layer, hidden layer (intermediate), and output layer. The neurons are the fundamental building blocks found within each layer. Fundamentally, for making connections between the layers, firstly, the transferring functions are applied, and, then, suitable algorithms are deployed to train the model [94]. The connections between the neurons are accompanied by weights and biases [95]. The AAN algorithm has two main steps: training and testing. The input parameters are transferred by the hidden layer to the output layer. Then, the testing step is conducted to compare the predicted *ROP* values with the real field *ROP* data. The main disadvantage of the ANN algorithm is that it creates "black box" models, meaning that there is no way to express how the results were obtained. Another demerit is that a large number of variables must be set in the neural network to prevent potential overtraining [96].

The first ANN study for predicting the rate of penetration was provided by Bilgesu et al. [97]. Then, Anemangely et al. devised two hybrid ANN models to develop an applicable *ROP* model [33]. Another ANN-based model was developed by Elkatatny [34]. The results of such research were found to be highly accurate. Jahanbakshi developed an ANN model to predict the *ROP* in oil and gas wells. The model was reported as a strongly reliable estimator capable of predicting precise results. Furthermore, some researchers applied other ANN architectures, such as back propagation neural networks (BPNN) [29] and the extreme learning machine (ELM) [98,99], for *ROP* prediction. The ELM approach was reported as a more accurate estimator in comparison to the ANN model [98,99].

As well as the ANN approach, the SVM algorithm has been successfully adopted in *ROP* modeling tasks. SVM is a supervised machine-learning algorithm which uses an ε-insensitive loss function. Bodaghi et al. compared the performance of SVM with the BPNN algorithm in *ROP* prediction. It was found that the SVM model was more accurate than the BPNN model [100]. Abdulmalek et al. used the SVM technique for *ROP* prediction [37]. Furthermore, other SVM-based approaches, such as the least-squares support-vector regression (LS-SVR) model, have been applied in *ROP* modeling. In another research, Ahmed at al. compared the performance of ANN, ELM, SVM, and LS-SVR algorithms in *ROP* prediction for two on-shore wells in the Niger Delta. It was reported that the LS-SVR and SVM models showed better performance than the ANN and ELM counterparts; however, the testing time required for the LS-SVR and SVM algorithms was much higher than the ANN and ELM approaches [99].

Apart from the neural networks and SVM-based algorithms, some researchers have utilized hybrid approaches to predict the *ROP* in their works. As a newly conducted research, Sobhi attempted to establish an *ROP* predictive model based on the previous empirical *ROP* models [35]. In such research, several algorithms (fminsearch, fsolve, fminunc, lsqcurvefit, lsqnonlin ant colony optimization (ACO), and multiple regression) and different objective functions were applied. Moreover, Mantha and Samuel combined several AI methods with the statistical regression technique to estimate the *ROP* [36]. Furthermore, Hegde et al. applied some hybrid models for *ROP* modeling [38]. In addition, Yavari et al. employed neuro-fuzzy technique to analyze *ROP* data [39]. In a recent study, Gan et al. combined the SVM, mutual information analysis, and wavelet filtering to create a hybrid *ROP* model [40].

Selecting an appropriate AI algorithm for the purpose of *ROP* prediction can be a challenging task. In better words, there is no standard procedure or reference to choose the best AI algorithm for *ROP* prediction. For instance, although the linear regression is computationally simple, it is not reliable in case of the presence of delimited parameters [101].

Other examples are decision trees, which exhibit noticeable accuracy even in the presence of outliers and noise; however, their results may be affected by unwanted overfitting.

As shown in Table 3, the number and type of input parameters are very inconsistent in different researches. Thus, even if the most optimal AI algorithm is selected, the determination of the optimal number of input parameters remains still challenging. Moreover, the type of input parameters can remarkably affect the accuracy of the results predicted by the applied AI technique [102]. It is noteworthy that the drilling operations are executed in geologically different formations, such as sandstone, shade, limestone, etc. Hence, the in situ lithology can closely determine the selection of number and type of the input parameters. As the geological parameters may exhibit intense fluctuations with depth, the presence of outliers or noisy data is inevitable. Therefore, the capability of the selected AI algorithm in prevention of such impacts must be taken into account. Generally, the statistical regression techniques are more affected by noisy data compared to the neural networks. Nevertheless, neural networks are more sensitive to noisy data when compared to SVM-based models.

Even more than this, the user-entered ratio of training data to the testing data may affect the results [102]. The optimal ratio may be obtained by the trial-and-error process which is time-consuming and inconsistent, depending on different cases.

Table 3. Some major studies related to *ROP* prediction by AI techniques.

Reference	AI Technique	Input Parameters
Bilgesu, 1997 [97]	ANN	drillability; formation abrasiveness; rotary time; bearing wear; torque; tooth wear; *WOB*; pump rate; *RPM*.
Moran, 2010 [103]	ANN	formation strength; formation abrasiveness; bit weight; *RPM*; drilling fluid weight; rock gense.
Jahanbakhshi, 2012 [29]	ANN	mud type; pressure differential; hydraulic power of the bit; hydraulics; bit wear; depth; *RPM*; pump pressure; *WOB*; formation density; bit type; ECD; 10 min gel strength of drilling fluid; wellbore diameter; early gel strength of drilling fluid; drillability; drilling fluid's yield point; permeability; drilling fluid's plastic viscosity; porosity.
Amar and Ibrahim, 2012 [79]	ANN	pore fluid pressure; *RPM*; depth; ECD; Reynolds number function; tooth wear; *WOB*.
Alarfaj et al., 2012 [104]	ANN	Reynolds number; depth; *WOB*; *RPM*; tooth wear; gradient of pore pressure; ECD.
Cui et al., 2014 [105]	ANN	apparent viscosity; unconfined compressive strength; mud density; *RPM*; bit geometry; *WOB*; bit type; gross hours drilled; drillability constant.
Bodaghi, 2015 [100]	SVM	viscosity; mud weight; tooth wear; pump rate; bit geometry; formation; deviation of well; *RPM*; depth.
Mantha and Samuel, 2016 [36]	Hybrid system	*RPM*; flow rate; *WOB*.
Shi et al., 2016 [99]	ANN, ELM	mud properties; formation; *RPM*; geomechanical characteristics; *WOB*; hydraulics.
Amer, 2017 [106]	ANN	*WOB*; mud weight; bit gense; mineralogy; IADC codes; drill-pipe pressure; bit size; mud pump; bit condition; torque; depth; *RPM*; TVD.
Abdulmalek et al., 2018 [37]	SVM	yield point; *WOB*; solid; *RPM*; funnel viscosity; flow rate; plastic viscosity; standpipe pressure; mud density; torque.
Yavari et al., 2018 [39]	Hybrid system	*WOB* and *RPM*.
Anemangely, 2018 [33]	Hybrid system	*RPM*; *WOB*; shear wave slowness; compressional wave slowness; flow rate.
Ahmed et al., 2018 [99]	ANN, ELM, SVM, and LS-SVR	depth; flow rate; *WOB*; *RPM*; torque; standpipe pressure; mud weight; bit diameter.
Hegde et al., 2018 [38]	Hybrid system	*RPM*; UCS; flow rate; *WOB*.

Table 3. *Cont.*

Reference	AI Technique	Input Parameters
Gan et al., 2019 [40]	ANN	seismic velocity; depth; torque; *WOB*; *RPM*; drillability; depth; mud density.
Elkatatny, 2021 [107]	Hybrid system	UCS; *WOB*; drill-pipe pressure; *RPM*; flow rate; torque; mud density; gamma ray; bit design; total flow area.
Lawal, 2021 [108]	ANN	density; porosity; point load index.
Mahdi, 2021 [98]	ANN	flow rate; *WOB*; *RPM*; bit diameter; standpipe pressure.
Sobhi et al., 2022 [35]	Hybrid system	depth; Reynolds number; *WOB*; tooth wear; ECD; *RPM*.

4. Discussion

Over the past few decades, drilling engineers have dealt with *ROP* prediction to heighten drilling efficiency [109]. More complicated wells must be drilled since access to hydrocarbon reservoirs is getting harder due to the deeper formations and increasing geologically problematic conditions. In order to increase drilling efficiency, precise prediction of the *ROP* has become more critical. This allows drilling engineers to accurately evaluate associated expenditure, required time, and proper phasing of the drilling operations.

Since the relationships between the factors affecting the *ROP* are quite complicated, a number of empirical and data-driven *ROP* predictive models have already been developed. Each *ROP* model has its own advantages and disadvantages. Therefore, there is no unique *ROP* model which is applicable for all circumstances. The empirical *ROP* models were developed mainly based on field experience and observations. Hence, the working experience of researchers influenced the number and type of factors considered in the empirical *ROP* models. On the opposite side, although powerful AI techniques, such as ANN and SVM algorithms, formulate the *ROP* without prior assumptions, they are highly sensitive to the number and type of input parameters. Thus, one potential solution is to develop formation-classified *ROP* models in which the number and type of contributing factors are determined for specific rock classes. In the oil and gas industry, the main rock types are sedimentary formations, including sandstones, shales, limestones, dolomites, and evaporated rocks [110]. If such formation-based *ROP* models are developed, the *ROP* values can be accurately predicted using the minimum number of effective parameters. For instance, rock abrasiveness can be classified as a highly influencing factor in *ROP* predictive models for sandstones, but not for evaporative rocks. By contrast, rock creep is of paramount importance in *ROP* models for evaporative rocks, but not for sandstone formations.

Drilling a directional well costs from 1.4 to 3 times more than a vertical well. Hence, for directional drilling operations, the *ROP* prediction must be calculated more carefully. Among the empirical *ROP* models, only Osguei's [68] considered the effect of wellbore inclination on the *ROP*. On the other hand, since the study refers to 15 years ago and drilling technology has advanced remarkably since then, the inclusion of wellbore inclination in current *ROP* models is of paramount urgency.

Future *ROP* models need further inclusion of uncontrollable factors, such as rock permeability, wellbore inclination, temperature, and rock hardness. In addition to these rock characteristics, the impact of discontinuities on the *ROP* can be further investigated. Fowell and Mcfeat-Smith in Ref. [111] discovered that when joint spacing reduces, the penetration rates rise. Moreover, Willbur in Ref. [112] proposed a classification to quantify the drillability of different rocks based on the rock composition and the characteristics of discontinuities. Also, Hoseinie et al. in Ref. [50] created a categorization system based on the texture and grain size, Mohs hardness, UCS, joint spacing, joint filling, and joint dipping to evaluate the drillability of different rock masses.

5. Conclusions

In this research, an inclusive survey on existing *ROP* models was conducted. The focus was on the elaboration of up-to-date investigations, current shortcomings, and future requirements. To do this, firstly, the contributing factors on the *ROP* were explained. Then, the different empirical and data-driven *ROP* models were elaborated, and their input parameters, assumptions, applicabilities, and drawbacks were described. Assessment of existing *ROP* models revealed that only 27% of the investigated contributing parameters were uncontrollable factors. Those uncontrollable factors are mostly related to the geological characteristics of the rocks. Furthermore, the frequency analysis of the input parameters showed that four uncontrollable factors, including rock permeability, wellbore inclination, rock hardness, and temperature, have not been adequately incorporated into the *ROP* predictive models. Among these factors, the wellbore inclination is more critical as the majority of the today's wellbores are drilled directionally. Hence, the modification of previous *ROP* models for inclined wellbores appears to be much needed. For this purpose, different experimental and numerical modelings should be carried out to investigate the *ROP* variations for inclined wellbores. In such inclined wellbores, the bottom-hole cleaning parameters, such as the coefficient of cuttings concentration and modified directional *WOB*, must be studied.

Generally, empirical *ROP* models are limited by different assumptions. Moreover, they may need experimental coefficients which can affect the results. Comparing the empirical and AI-based *ROP* models, it can be said that the application of data-driven models can markedly enhance the accuracy of the predicted *ROP* values. These models consider no operational assumption in their computational processes. Furthermore, numerous controllable and uncontrollable variables can be imported to such models. However, different AI techniques, such as ANN, SVM, decision tree, etc., may display different accuracy levels, especially for different lithology conditions. As a matter of fact, lithology is remarkably influential in the quality of the data gathered during the drilling operations; in some lithology, the different geological parameters can be accompanied by different levels of noisy data and outliers. Thus, the sensitivity of different AI algorithms to noisy data and outliers must be considered during the development of data-driven *ROP* models.

The size and type of the input parameters can also impact the accuracy of data-driven *ROP* models. To address this issue, it is suggested to develop a formation-based classification system in which the type of the contributing factors is determined for drilling different formations. Such formation-based classification systems have already been developed for geomechanical investigations. For instance, the rock mass rating (RMR) system was proposed by Bieniawski for the excavation of tunnels in different rocks [113]. Another illustration is the Q-System developed by Bartun et al. for the design of underground excavations [114]. Both RMR and the Q-System are in the form of tables in which different geological conditions of rocks have been quantified. Therefore, drilling/geomechanics engineers can convert the qualitative geological properties into quantitative numbers. Those numbers are then used for classification of rocks.

The findings of this research are quite practical for the future investigations on *ROP* prediction. Moreover, it benefits the companies and organizations dealing with drilling operations in petroleum engineering, mining engineering, space engineering, and water-well drilling.

Author Contributions: Conceptualization, D.K. and M.K.; methodology, D.K. and M.K.; software, M.K.; validation, D.K.; formal analysis, D.K.; investigation, M.K.; resources, M.K. and D.K.; data curation, M.K.; writing—original draft preparation, M.K. and D.K.; writing—review and editing, D.K. and M.K.; visualization, M.K. and D.K.; supervision, D.K.; project administration, D.K.; funding acquisition, D.K. All authors have read and agreed to the published version of the manuscript.

Funding: The project was supported by the AGH University of Krakow, Poland. subsidy 16.16.190.779.

Institutional Review Board Statement: Not applicable.

Informed Consent Statement: Not applicable.

Data Availability Statement: All used data are accessible in the context of the article.

Conflicts of Interest: The authors declare no conflict of interest.

References

1. De Oliveira, L.S.R.; Nascimento, A.; Mantegazini, D.Z.; Nascimento, N. Drilling optimization of petroleum wells: A data analysis of the drilling fluid flow-rate influence in *ROP*. *Lat. Am. J. Energy Res.* **2021**, *8*, 59–66. [CrossRef]
2. Bourgoyne, A.T.; Millheim, K.K.; Chenevert, M.E.; Young, F.S. *Applied Drilling Engineering*; Society of Petroleum Engineers Richardson: Richardson, TX, USA, 1986.
3. Bourgoyne, A.T.; Young, F.S. A Multiple Regression Approach to Optimal Drilling and Abnormal Pressure Detection. *Soc. Pet. Eng. J.* **1974**, *14*, 371–384. [CrossRef]
4. Youcefi, M.R.; Hadjadj, A.; Bentriou, A.; Boukredera, F.S. Rate of penetration modeling using hybridization extreme learning machine and whale optimization algorithm. *Earth Sci. Inform.* **2020**, *13*, 51–68. [CrossRef]
5. Edalatkhah, S.; Rasoul, R.; Hashemi, A. Bit selection optimization using artificial intelligence systems. *Pet. Sci. Technol.* **2010**, *28*, 1946–1956. [CrossRef]
6. Protodyakonov, M.M. Mechanical properties and drillability of rocks. In *Proceedings of the 5th Symposium Rock Mechanics*; University of Minnesota: Minneapolis, MN, USA, 1963.
7. Paone, J.; Madson, D.; Bruce, W.E. *Drillability Studies-Laboratory Percussive Drilling*; No. 7300-7309; US Department of the Interior, Bureau of Mines: Washington, DC, USA, 1969.
8. Tandanand, S.; Unger, H.F. *Drillability Determination: A Drillability Index for Percussion Drills*; US Department of the Interior, Bureau of Mines: Washington, DC, USA; University of Michigan: Ann Arbor, MI, USA, 1975; Volume 8073.
9. Pathankar, G.B.; Misra, A. critical appraisal of the Protodyakonov Index. *Int. J. Rock Mech. Min. Sci.* **1976**, *13*, 249–251. [CrossRef]
10. Rabia, H. *Oilwell Drilling Engineering: Principles and Practise*; Graham & Tromtman: Gaihersburg, MD, USA, 1985.
11. Bond, D.F. The optimization of PDC bit selection using sonic velocity profiles present in the Timor Sea. *SPEDE* **1990**, *5*, 135–142.
12. Perrin, V.P.; Mensa-Wilmot, G.; Alexander, W.L. Drilling index-a new approach to bit performance evaluation. In Proceedings of the SPE/IADC Drilling Conference, Amsterdam, The Netherlands, 4–6 March 1997. [CrossRef]
13. Graham, J.W.; Muench, N.L. Analytical determination of optimum bit weight and rotary speed combinations. In Proceedings of the in Fall Meeting of the Society of Petroleum Engineers of AIME, Dallas, TX, USA, 4–7 October 1959. [CrossRef]
14. Maurer, W.C. The "Perfect—Cleaning" Theory of Rotary Drilling. *J. Pet. Technol.* **1962**, *14*, 1270–1274. [CrossRef]
15. Galle, H.B.; Woods, E.M. Best Constant Weight and Rotary Speed for Rotary Rock Bits. Hughes Tool, Co.: New York, NY, USA, 1963.
16. Bingham, M.G. *A New Approach to Interpreting Rock Drill-Ability*; Petroleum Pub. Co.: Oklahoma, OK, USA, 1965.
17. Teale, R. The Concept of Specific Energy in Rock Drilling. *Int. J. Rock Mech. Min.* **1965**, *2*, 57–73. [CrossRef]
18. Eckel, J.R. Microbit studies of the effect of fluid properties and hydraulics on drilling rate. *J. Pet. Technol.* **1967**, *19*, 541–546. [CrossRef]
19. Eren, T.; Ozbayoglu, M.E. Real-time drilling rate of penetration performance monitoring. In Proceedings of the Offshore Mediterranean Conference and Exhibition, Ravenna, Italy, 23 March 2011.
20. Warren, T.M. Drilling Model for Soft-Formation Bits. *J. Pet. Technol.* **1981**, *33*, 963–970. [CrossRef]
21. Warren, T.M. Factors Affecting Torque for a Roller Cone Bit. *J. Pet. Technol.* **1984**, *36*, 1500–1508. [CrossRef]
22. Al-Betairi, E.A.; Moussa, M.M.; Al-Otaibi, S. Multiple regression approach to optimize drilling operations in the Arabian Gulf area. *SPE Drill. Eng.* **1988**, *3*, 83–88. [CrossRef]
23. Maidla, E.E.; Ohara, S. Field Verification of Drilling Models and Computerized Selection off Drill Bit, *WOB*, and Drillstring Rotation. *SPE Drill. Eng.* **1991**, *6*, 189–195. [CrossRef]
24. Hareland, G.; Rampersad, P.R. Drag-bit model including wear. In Proceedings of the SPE Latin America/Caribbean Petroleum Engineering Conference, Buenos Aires, Argentina, 27–29 April 1994. [CrossRef]
25. Motahhari, H.R.; Hareland, G.; James, J.A. Improved drilling efficiency technique using integrated PDM and PDC bit parameters. *J. Can. Pet. Technol.* **2010**, *49*, 45–52. [CrossRef]
26. Hareland, G.; Wu, A.; Rashidi, B.; James, J.A. A new drilling rate model for tricone bits and its application to predict rock compressive strength. In Proceedings of the 44th US Rock Mechanics Symposium and 5th US-Canada Rock Mechanics Symposium, Salt Lake City, UT, USA, 27 June 2010.
27. Alum, M.A.; Egbon, F. Semi-analytical models on the effect of drilling fluid properties on rate of penetration (*ROP*). In Proceedings of the Nigeria Annual International Conference and Exhibition, Abuja, Nigeria, 30 July–3 August 2011. [CrossRef]
28. Moazzeni, A.R.; Khamehchi, E. Rain optimization algorithm (roa): A new metaheuristic method for drilling optimization solutions. *J. Pet. Sci. Eng.* **2020**, *195*, 107512. [CrossRef]
29. Jahanbakhshi, R.; Keshavarzi, R.; Jafarnezhad, A. Real-time prediction of rate of penetration during drilling operation in oil and gas wells. In Proceedings of the 46th US Rock Mechanics/Geomechanics Symposium, Chicago, IL, USA, 24 June 2012.
30. Bataee, M.; Irawan, S.; Kamyab, M. Artificial neural network model for prediction of drilling rate of penetration and optimization of parameters. *J. Jpn. Pet. Inst.* **2014**, *57*, 65–70. [CrossRef]
31. Kahraman, S. Estimating the Penetration Rate in Diamond Drilling in Laboratory Works Using the Regression and Artificial Neural Network Analysis. *Neural Process. Lett.* **2016**, *43*, 523–535. [CrossRef]
32. Hegde, C.; Daigle, H.; Millwater, H.; Gray, K. Analysis of Rate of Penetration (*ROP*) Prediction in Drilling Using Physics-Based and Data-Driven Models. *J. Pet. Sci. Eng.* **2017**, *159*, 295–306. [CrossRef]

33. Anemangely, M.; Ramezanzadeh, A.; Tokhmechi, B.; Molaghab, A.; Mohammadian, A. Drilling rate prediction from petrophysical logs and mud logging data using an optimized multilayer perceptron neural network. *J. Geophys. Eng.* **2018**, *15*, 1146–1159. [CrossRef]
34. Elkatatny, S. Development of a new rate of penetration model using self-adaptive differential evolution-artificial neural network. *Arab. J. Geosci.* **2019**, *12*, 19. [CrossRef]
35. Sobhi, I.; Dobbi, A.; Hachana, O. Prediction and analysis of penetration rate in drilling operation using deterministic and metaheuristic optimization methods. *J. Pet. Explor. Prod. Technol.* **2022**, *12*, 1341–1352. [CrossRef]
36. Mantha, B.; Samuel, R. ROP optimization using artificial intelligence techniques with statistical regression coupling. In Proceedings of the SPE Annual Technical Conference and Exhibition, Dubai, UAE, 26–28 September 2016. [CrossRef]
37. Abdulmalek, A.S.; Salaheldin, E.; Abdulazeez, A.; Mohammed, M.; Abdulwahab, Z.A.; Mohamed, I.M. Prediction of rate of penetration of deep and tight formation using support vector machine. In Proceedings of the SPE Kingdom of Saudi Arabia Annual Technical Symposium and Exhibition, Dammam, Saudi Arabia, 23 April 2018. [CrossRef]
38. Hegde, C.; Soares, C.; Gray, K. September. Rate of penetration (ROP) modeling using hybrid models: Deterministic and machine learning. In Proceedings of the Unconventional Resources Technology Conference, Houston, TX, USA, 23–25 July 2018. [CrossRef]
39. Yavari, H.; Sabah, M.; Khosravanian, R.; Wood, D. Application of an adaptive neuro-fuzzy inference system and mathematical rate of penetration models to predicting drilling rate. *Iran. J. Oil Gas Sci. Technol.* **2018**, *7*, 73–100. [CrossRef]
40. Gan, C.; Cao, W.; Wu, M.; Liu, K.Z.; Chen, X.; Hu, Y.; Ning, F. Two-level intelligent modeling method for the rate of penetration in complex geological drilling process. *Appl. Soft Comput.* **2019**, *80*, 592–602. [CrossRef]
41. Dunlop, J.; Isangulov, R.; Aldred, W.D.; Sanchez, H.A.; Flores, J.L.; Herdoiza, J.A.; Belaskie, J.; Luppens, J.C. Increased rate of penetration through automation. In Proceedings of the SPE/IADC Drilling Conference and Exhibition, Amsterdam, The Netherlands, 1–3 March 2011. [CrossRef]
42. Stelzer, C. *Drillpipe Failure and Its Prediction Doctoral Dissertation*; University of Leoben: Leoben, Austria, 2007.
43. Hegde, C.; Gray, K.E. Use of Machine Learning and Data Analytics to Increase Drilling Efficiency for Nearby Wells. *J. Nat. Gas Sci. Eng.* **2017**, *40*, 327–335. [CrossRef]
44. Hoseinie, S.H.; Ataei, M.; Osanloo, M. A new classification system for evaluating rock penetrability. *Int. J. Rock Mech. Min. Sci.* **2009**, *46*, 1329–1340. [CrossRef]
45. Knez, D.; Calicki, A. Looking for a New Source of Natural Proppants in Poland. *J. Bull. Pol. Acad. Sci. Tech. Sci.* **2018**, *66*, 3–8. [CrossRef]
46. Knez, D.; Mazur, S. Simulation of Fracture Conductivity Changes due to Proppant Composition and Stress Cycles. *J. Pol. Miner. Eng. Soc.* **2019**, *2*, 231–234.
47. Niyazi, B. Determination of drillability of some natural stones and their association with rock properties. *Sci. Res. Essays* **2011**, *6*, 382–387. [CrossRef]
48. Kuesel, T.R.; King, E.H.; Bickel, J.O. *Tunnel Engineering Handbook*; Springer Science & Business Media: Berlin/Heidelberg, Germany, 2012.
49. Howarth, D.F. Experimental study on the relationship between rock texture and mechanical performance. *Trans. Inst. Min. Metall. Sect. A* **1986**, *95*, 41–45.
50. Hoseinie, S.H.; Aghababaei, H.; Pourrahimian, Y. Development of a new classification system for assessing of rock mass drillability index (RDi). *Int. J. Rock Mech. Min. Sci.* **2008**, *45*, 1–10. [CrossRef]
51. Knez, D.; Wiśniowski, R.; Owusu, W.A. Turning Filling Material into Proppant for Coalbed Methane in Poland—Crush Test Results. *Energies* **2019**, *12*, 1820. [CrossRef]
52. Kumar, S.; Murthy, V.M.S.R. Experimental studies on drill penetration rate prediction in coal measure rocks through Cerchar hardness index tests. *J. Mines Met. Fuels* **2014**, *62*, 88–95. [CrossRef]
53. Kumar, S.; Murthy, V.M.S.R. Predicting penetration rate for rotary blast hole drills in surface coal mines—An approach. In Proceedings of the 6th National Seminar on Surface Mining (NSSM), Indian School of Mines, Dhanbad, India, 10–11 January 2014.
54. Khalilidermani, M.; Knez, D.; Zamani, M.A.M. Empirical Correlations between the Hydraulic Properties Obtained from the Geoelectrical Methods and Water Well Data of Arak Aquifer. *Energies* **2021**, *14*, 5415. [CrossRef]
55. Knez, D.; Rajaoalison, H. Land Subsidence Assessment for Wind Turbine Location in the South-Western Part of Madagascar. *Energies* **2022**, *15*, 4878. [CrossRef]
56. Knez, D.; Khalilidermani, M. A Review of Different Aspects of Off-Earth Drilling. *Energies* **2021**, *14*, 7351. [CrossRef]
57. Knez, D.; Zamani, M.A.M. A Review of the Geomechanics Aspects in Space Exploration. *Energies* **2021**, *14*, 7522. [CrossRef]
58. Mitchell, R.F.; Miska, S.Z. *Fundamentals of Drilling Engineering*; Society of Petroleum Engineers: Richardson, TX, USA, 2011; ISBN 978-1-61399-951-6. [CrossRef]
59. Hossain, M.E.; Al-Majed, A.A. *Fundamentals of Sustainable Drilling Engineering*; Wiley: Hoboken, NJ, USA, 2015; pp. 374–412. [CrossRef]
60. Knez, D.; Khalilidermani, M.; Zamani, M.A.M. Water Influence on the Determination of the Rock Matrix Bulk Modulus in Reservoir Engineering and Rock-Fluid Coupling Projects. *Energies* **2023**, *16*, 1769. [CrossRef]
61. Knez, D.; Zamani, M.A.M. Empirical Formula for Dynamic Biot Coefficient of Sandstone Samples from South-West of Poland. *Energies* **2021**, *14*, 5514. [CrossRef]

62. Zamani, M.A.M.; Knez, D. A New Mechanical-Hydrodynamic Safety Factor Index for Sand Production Prediction. *Energies* **2021**, *14*, 3130. [CrossRef]
63. Rajaoalison, H.; Knez, D.; Zlotkowski, A. Changes of Dynamic Mechanical Properties of Brine-Saturated Istebna Sandstone under Action of Temperature and Stress. *Przemysł Chem.* **2019**, *98*, 801–804.
64. Knez, D.; Rajaoalison, H. Discrepancy between Measured Dynamic Poroelastic Parameters and Predicted Values from Wyllie's Equation for Water-Saturated Istebna Sandstone. *Acta Geophys.* **2021**, *69*, 673–680. [CrossRef]
65. Young, F.S., Jr. Computerized Drilling Control. *J. Pet. Technol.* **1969**, *21*, 483–496. [CrossRef]
66. Reza, M.R.; Alcocer, C.F. A unique computer simulation model well drilling: Part I-the reza drilling model. In Proceedings of the SPE California Regional Meeting, Oakland, CA, USA, 2–4 April 1986. [CrossRef]
67. Ziaja, M.B.; Miska, S. Mathematical model of the diamond-bit drilling process and its practical application. *Soc. Pet. Eng. J.* **1982**, *22*, 911–922. [CrossRef]
68. Osgouei, R.E. *Rate of Penetration Estimation Model for Directional and Horizontal Wells*; Middle East Technical University: Ankara, Turkey, 2007.
69. Kirencigil, E. *Numerical Modelling of the Hydraulic of the Drilling Process Using PDC Drill Bit*; Graduate Faculty of the University of Akron: Akron, OH, USA, 2017.
70. Boyun, G.; Gefei, L. *Applied Drilling Circulation Systems (Hydraulic, Calculations and Models)*; Gulf Publishing Company: Houston, TX, USA, 2011; ISBN 978-0-12-381957-4.
71. Langston, J.W. A Methtid of Utilizing Existing Information To optimize Drilling Procedures. *J. Pet. Technol.* **1966**, *18*, 677–686. [CrossRef]
72. Khalilidermani, M.; Knez, D. A Survey of Application of Mechanical Specific Energy in Petroleum and Space Drilling. *Energies* **2022**, *15*, 3162. [CrossRef]
73. Nearly All New U.S. Crude Oil and Natural Gas Wells Are Horizontal or Directional. Available online: https://www.eia.gov/todayinenergy/detail.php?id=52138 (accessed on 15 March 2023).
74. Miska, S.Z.; Mitchell, R.F.; Ozbayoglu, E.M. *Drilling Engineering: Advanced Applications and Technology*, 1st ed.; McGraw Hill: New York, NY, USA, 2022.
75. Chen, X.; Fan, H.; Guo, B.; Gao, D.; Wei, H.; Ye, Z. Real-time prediction and optimization of drilling performance based on a new mechanical specific energy model. *Arab. J. Sci. Eng.* **2014**, *39*, 8221–8231. [CrossRef]
76. Hardness and Toughness of Rocks. Available online: https://www.911metallurgist.com/hardness-toughness-rocks/ (accessed on 11 April 2023).
77. Mendes, J.R.P.; Fonseca, T.C.; Serapião, A. Applying a genetic neuro-model reference adaptive controller in drilling optimization. *World Oil* **2007**, *228*, 29–36.
78. Paiaman, A.M.; Al-Askari, M.G.; Salmani, B.; Al-Anazi, B.D.; Masihi, M. Effect of drilling fluid properties on rate of penetration. *Nafta* **2009**, *60*, 129–134.
79. Amar, K.; Ibrahim, A. Rate of Penetration Prediction and Optimization Using Advances in Artificial Neural Networks, a Comparative Study. In Proceedings of the 4th International Joint Conference on Computational Intelligence, Barcelona, Spain, 5–7 October 2012; SciTePress—Science and Technology Publications: Barcelona, Spain, 2012; pp. 647–652.
80. Sultan, M.A.; Al-Kaabi, A.U. Application of neural network to the determination of well-test interpretation model for horizontal wells. In Proceedings of the SPE Asia Pacific Oil and Gas Conference and Exhibition, Melbourne, Australia, 8–10 October 2002. [CrossRef]
81. Abtahi, A. Bit Wear Analysis and Optimization for Vibration Assisted Rotary Drilling (VARD) Using Impregnated Diamond Bits. Doctoral Dissertation, Memorial University of Newfoundland, St. John's, NL, Canada, 2011.
82. Hamrick, T.R. *Optimization of Operating Parameters for Minimum Mechanical Specific Energy in Drilling*; West Virginia University: Morgantown, WV, USA, 2011.
83. Bahari, A.; Baradaran Seyed, A. Drilling cost optimization in a hydrocarbon field by combination of comparative and mathematical methods. *Pet. Sci.* **2009**, *6*, 451–463. [CrossRef]
84. Anemangely, M.; Ramezanzadeh, A.; Tokhmechi, B. Determination of constant coefficients of Bourgoyne and Young drilling rate model using a novel evolutionary algorithm. *J. Min. Environ.* **2017**, *8*, 693–702. [CrossRef]
85. Elkatatny, S. New approach to optimize the rate of penetration using artificial neural network. *Arab. J. Sci. Eng.* **2018**, *43*, 6297–6304. [CrossRef]
86. Minghui, W.; Gensheng, L.; Huaizhong, S.; Shuaishuai, S.; Zhaokun, L.; Yi, Z. Theories and Applications of Pulsed-Jet Drilling with Mechanical Specific Energy. *SPE J.* **2016**, *21*, 303–310. [CrossRef]
87. Dupriest, F.E.; Koederitz, W.L. Maximizing Drill Rates with Real-Time Surveillance of Mechanical Specific Energy. In Proceedings of the SPE Annual Technical Conference and Exhibition, Amsterdam, The Netherlands, 23 February 2005.
88. Knez, D. Stress State Analysis in Aspect of Wellbore Drilling Direction. *Arch. Min. Sci.* **2014**, *59*, 71–76. [CrossRef]
89. Bello, O.; Teodoriu, C.; Yaqoob, T.; Oppelt, J.; Holzmann, J.; Obiwanne, A. Application of artificial intelligence techniques in drilling system design and operations: A state of the art review and future research pathways. In Proceedings of the SPE Nigeria Annual International Conference and Exhibition, Lagos, Nigeria, 2–4 August 2016. [CrossRef]
90. Pollock, J.; Stoecker-Sylvia, Z.; Veedu, V.; Panchal, N.; Elshahawi, H. Machine learning for improved directional drilling. In Proceedings of the Offshore Technology Conference, Houston, TX, USA, 30 April–3 May 2018. [CrossRef]

91. Zakharov, L.A.; Martyushev, D.A.; Ponomareva, I.N. Predicting dynamic formation pressure using artificial intelligence methods. *J. Min. Inst.* **2022**, *253*, 23–32. [CrossRef]
92. Angelini, E.; Ludovici, A. CDS evaluation model with neural networks. *J. Serv. Sci. Manag.* **2009**, *2*, 15. [CrossRef]
93. Monjezi, M.; Dehghani, H. Evaluation of effect of blasting pattern parameters on back break using neural networks. *Int. J. Rock Mech. Min. Sci.* **2008**, *45*, 1446–1453. [CrossRef]
94. Lippmann, R.P. An introduction to computing with neural nets. *IEEE Assp Mag.* **1987**, *4*, 4–22. [CrossRef]
95. Hinton, G.E.; Osindero, S.; Teh, Y.W. A fast learning algorithm for deep belief nets. *Neural Comput.* **2006**, *18*, 1527–1554. [CrossRef]
96. Ahmed, O.; Adeniran, A.; Samsuri, A. *Drilling*; Intech Open: London, UK, 2018. [CrossRef]
97. Bilgesu, H.I.; Tetrick, L.T.; Altmis, U.; Mohaghegh, S.; Ameri, S. A New Approach for the Prediction of Rate of Penetration (*ROP*) Values. In Proceedings of the SPE Annual Technical Conference and Exhibition, Lexington, KY, USA, 22 October 1997; p. SPE-39231-MS.
98. Mahdi, D.S. Predicting Drilling Rate of Penetration Using Artificial Neural Networks. In Proceedings of the 4th International Conference on Engineering Sciences (ICES 2020), Kerbala, Iraq, 5–6 December 2020. [CrossRef]
99. Shi, X.; Liu, G.; Gong, X.; Zhang, J.; Wang, J.; Zhang, H. An efficient approach for real-time prediction of rate of penetration in offshore drilling. *Math. Probl. Eng.* **2016**, *2016*, 3575380. [CrossRef]
100. Bodaghi, A.; Ansari, H.R.; Gholami, M. Optimized support vector regression for drillingrate of penetration estimation. *Open Geosci.* **2015**, *7*, 870–879. [CrossRef]
101. Noshi, C.I.; Schubert, J.J. The role of machine learning in drilling operations; a review. In Proceedings of the SPE/AAPG Eastern Regional Meeting, Pittsburgh, PA, USA, 7–11 October 2018. [CrossRef]
102. Mostafaei, K.; Maleki, S.; Mahmoudi, M.Z.A.; Knez, D. Risk management prediction of mining and industrial projects by support vector machine. *Resour. Policy* **2022**, *78*, 102819. [CrossRef]
103. Moran, D.; Ibrahim, H.; Purwanto, A.; Osmond, J. Sophisticated ROP prediction technologies based on neural network delivers accurate drill time results. In Proceedings of the IADC/SPE Asia Pacific Drilling Technology Conference and Exhibition, Ho Chi Minh City, Vietnam, 1–3 November 2010. [CrossRef]
104. AlArfaj, I.; Khoukhi, A.; Eren, T. Application of advanced computational intelligence to rate of penetration prediction. In Proceedings of the in UKSim/AMSS European Symposium on Computer Modeling and Simulation, Malta, Malta, 14–16 November 2012. [CrossRef]
105. Cui, M.; Sun, M.C.; Zhang, J.; Kang, K.; Luo, Y. Maximizing drilling performance with real-time surveillance system based on parameters optimization algorithm. *Adv. Pet. Explor. Dev.* **2014**, *8*, 15–24.
106. Amer, M.M.; Dahab, A.S.; El-Sayed, A.A.H. An ROP predictive model in Nile delta area using artificial neural networks. In Proceedings of the SPE Kingdom of Saudi Arabia Annual Technical Symposium and Exhibition, Dammam, Saudi Arabia, 24–27 April 2017. [CrossRef]
107. Elkatatny, S. Real-time prediction of rate of penetration while drilling complex lithologies using artificial intelligence techniques. *Ain Shams Eng. J.* **2021**, *12*, 917–926. [CrossRef]
108. Lawal, A.I.; Kwon, S.; Onifade, M. Prediction of rock penetration rate using a novel antlion optimized ANN and statistical modelling. *J. Afr. Earth Sci.* **2021**, *182*, 104287. [CrossRef]
109. Ansari, H.R.; Sarbaz Hosseini, M.J.; Amirpour, M. Drilling rate of penetration prediction through committee support vector regression based on imperialist competitive algorithm. *Carbonates Evaporites* **2017**, *32*, 205–213. [CrossRef]
110. Rajaoalison, H.; Knez, D.; Zamani, M.A.M. A Multidisciplinary Approach to Evaluate the Environmental Impacts of Hydrocarbon Production in Khuzestan Province, Iran. *Energies* **2022**, *15*, 8656. [CrossRef]
111. Fowell, R.J.; Mcfeat-Smith, I. Factors Influencing the Cutting Performance of a Selective Tunnelling Machine. In *Proceedings of the First International Symposium on Tunnelling*; Jones, J.M., Ed.; IMM: London, UK, 1976. Available online: https://pascal-francis.inist.fr/vibad/index.php?action=getRecordDetail&idt=PASCAL7780338404 (accessed on 11 April 2023).
112. Wilbur, L. Rock Tunnels. In *Tunnel Engineering Handbook*; Bichel, J.O., Kuesel, T.R., Eds.; Van Nostrand Reinhold Company: New York, NY, USA, 1982.
113. Bieniawski, Z.T. *Engineering Rock Mass Classifications: A Complete Manual for Engineers and Geologists in Mining, Civil, and Petroleum Engineering*; John Wiley & Sons: Hoboken, NJ, USA, 1989; pp. 40–47; ISBN 0-471-60172-1.
114. Barton, N.; Lien, R.; Lunde, J.J.R.M. Engineering classification of rock masses for the design of tunnel support. *Rock Mech.* **1974**, *6*, 189–236. [CrossRef]